Phase curve and albedo of asteroid 5535 Annefrank

Ray L. Newburn Jr.,[1] Thomas C. Duxbury, Martha Hanner, Boris V. Semenov, Edward E. Hirst, Ramachand S. Bhat, Shyamkumar Bhaskaran, Tseng-Chan M. Wang, and Peter Tsou
Jet Propulsion Laboratory, California Institute of Technology, Pasadena, California, USA

Donald E. Brownlee
Department of Astronomy, University of Washington, Seattle, Washington, USA

Allan R. Cheuvront, David E. Gingerich, Gregory R. Bollendonk, Joseph M. Vellinga, Kelly A. Parham, and Susan J. Mumaw
Lockheed Martin Astronautics, Denver, Colorado, USA

Received 17 April 2003; revised 2 July 2003; accepted 25 August 2003; published 12 November 2003.

[1] Seventy-two images of the S-class asteroid 5535 Annefrank, acquired on 2 November 2002 at target ranges of 11,415–3078.5 km, were transmitted to Earth as a part of an engineering readiness test of the Stardust mission. Forty-four of these were used to create a phase curve extending to 134°, the largest angle yet achieved for any S-class asteroid. Flux fell by more than six magnitudes between the extrapolated 0° and 134°. A maximum illuminated cross section of 16 km^2 was seen at a phase angle of 47.2°. Assuming a camera efficiency of 75%, a broadband (470–940 nm) geometric albedo of 0.24 was derived for Annefrank. *INDEX TERMS:* 6297 Planetology: Solar System Objects: Instruments and techniques; 6061 Planetology: Comets and Small Bodies: Remote sensing; 6205 Planetology: Solar System Objects: Asteroids and meteoroids; *KEYWORDS:* 5535 Annefrank, asteroid photometry, asteroid phase curves, asteroid imaging, asteroid albedos

Citation: Newburn, R. L., Jr., et al., Phase curve and albedo of asteroid 5535 Annefrank, *J. Geophys. Res.*, *108*(E11), 5117, doi:10.1029/2003JE002106, 2003.

1. Introduction

[2] On 2 November 2002 at 0451:20 UT the Stardust spacecraft flew past the asteroid Annefrank at a distance of 3078.5 km. The parameters of the flyby were established as those giving the best test of the spacecraft and its controlling software while minimizing risk to the primary mission objective of encountering Comet 81P/Wild 2 on 2 January 2004. In other words, this was strictly an engineering test, not a science activity, but nevertheless interesting science data were acquired. We report here on photometric properties of Annefrank.

2. Stardust Optical Navigation Camera

[3] The primary goal of the Stardust mission is to return cometary dust to Earth for study in terrestrial laboratories. A camera was included for purposes of optical navigation, which will be required to achieve a Wild 2 closest approach of roughly 150 km. The camera will be used to take science images of the comet nucleus during the flyby, but that goal is strictly secondary. The camera system consists of an f/3.5 Petzval type lens of 202 mm focal length with a 1024 × 1024 pixel CCD detector. These give a resolution of 59 μradians per pixel. The passband of the camera extends from 470 to 940 nm. No filters are available. There have been problems since launch with contamination of the optics from an unknown source. Most of this contamination has been removed from time to time with heating, but a shallow skirt of scattered light remains in the images, and considerable care must therefore be taken in their analysis. A detailed description of the camera and its current operational state can be found in the work of *Newburn et al.* [2003].

3. Imaging at Annefrank

[4] The most important goal of the Annefrank flyby was to test the Stardust autonomous encounter software. The spacecraft has to be able to control itself and keep its camera pointed at the target, without any human intervention, while 20 light minutes from Earth. The software is not bothered by overexposed (saturated) images, but there was concern that weak images could be a problem, especially if there were bright stars somewhere in the background field. Therefore, except for the 31 images taken nearest closest approach, exposure times were deliberately set high, and 22 of the 72 images transmitted to the ground contained saturated pixels. Thirty-four images were used by the spacecraft software without being stored for transfer to the

[1] Visiting from Chipton-Ross, Incorporated, Los Angeles, California, USA.

0148-0227/03/2003JE002106$09.00

Table 1. Log of Annefrank Images Taken by Stardust on 2 November 2002

Image (n0xxxae01)	Start Time, UT[a]	Exposure, ms	Distance to Annefrank, km	Phase Angle, deg	Integrated Uncompressed, dn	Normalized Integrated, dn/s	Mean Background, dn	Calculated Image Edge, dn	Comments
371	0426:01.678	65	11415	134.6	10,717	2,266,169	560.7		about 33% on periscope
372	0427:01.682	63.35	10997	134.0	9979	2,009,414	555.8	573.53	about 24% on periscope, severe smear
373	0428:01.682	65	10582	133.3	12,246.5	2,225,434	554.8	574.59	possibly 2–3% on periscope
374	0430:02.963	63.35	9747	131.8	15,806	2,500,333	554.6	576.26	
377	0431:02.685	65	9337	130.9	18,889.5	2,672,406	554.5	577.71	severe smear
380		63.35	8929	130.1					image very near edge
383	0433:02.689	65	8523	129.1	26,429	3,115,537	554.5	581.245	
386	0434:02.689	63.35	8120	128.0	32,045.5	3,518,140	554.3	583.879	severe smear
389	0435:02.689	65	7720	126.7	40,094	3,877,763	554.3	587.654	severe smear
392	0436:02.688	63.35	7325	125.4	462,07.5	4,128,210	554.3	590.521	
395		65	6933	123.9					image very near edge
398		63.35	6548	122.2					image very near edge
401		65	6168	120.3					image very near edge
404		63.35	5796	118.2					image blank except for one cosmic ray hit
407	0441:02.696	65	5434	115.7	223,384	10,704,308	553.9	673.617	severe smear
410	0442:02.696	23.35	5088	113.0	111,157	12,999,443	553.8	620.983	
413	0443:02.699	25	4744	109.8	177,763	16,879,957	553.8	652.221	
416	0444:02.699	23.35	4423	106.2	246,068	21,746,169	553.8	684.256	
417	0445:02.699	25	4123	102.0	398,273	28,565,916	553.9	755.640	
420		23.35	3848	97.1					first image with saturation
423		25	3605	91.6					
426		23.35	3402	85.5					
427		25	3384	84.8					image 80% saturated
428		23.35	3366	84.2					image >80% saturated
429		25	3349	83.5					image >80% saturated
430		23.35	3332	82.8					image >80% saturated
431		25	3315	82.1					image >80% saturated
432		23.35	3300	81.4					image >80% saturated
433		25	3284	80.7					image >80% saturated
434		23.35	3269	80.0					image >80% saturated
435		25	3255	79.3					image >80% saturated
436		23.35	3241	78.5					image >80% saturated
437		25	3228	77.8					image >80% saturated
438		23.35	3215	77.1					image >80% saturated
439		25	3203	76.3					image >80% saturated
440		23.35	3191	75.7					image >80% saturated
441		25	3180	74.8					image >80% saturated
442		23.35	3170	74.1					image >80% saturated

Table 1. (continued)

Image (n0xxxae01)	Start Time, UT[a]	Exposure, ms	Distance to Annefrank, km	Phase Angle, deg	Integrated Uncompressed, dn	Normalized Integrated, dn/s	Mean Background, dn	Calculated Image Edge, dn	Comments
443		25	3160	73.3					calculated; image >80% saturated
444		23.35	3150	72.5					illuminated; image >80% saturated
445		25	3141	71.8					area, km^2; image >80% saturated
446	0450:01.710	3.35	3133	71.0	306,672	94,783,061	552.8	712.68	15.7
447	0450:07.710	5	3125	70.2	476,233	98,113,811	553.2	792.20	15.6
448	0450:13.710	3.35	3118	69.4	321,406.5	98,388,127	552.8	719.59	15.6
449	0450:19.710	5	3111	68.6	498,808	101,846,017	553.4	802.79	15.5
450	0450:25.710	3.35	3105	67.8	338,864.5	102,869,137	553.0	727.78	15.4
451	0450:31.710	5	3100	67.1	520,364.5	105,497,378	553.1	812.90	15.4
452	0450:37.710	3.35	3095	66.3	356,877	107,640,494	553.0	736.23	15.3
453	0450:43.710	5	3090	65.5	54,7469	110,277,550	552.9	825.61	15.3
454	0450:49.710	3.35	3087	64.7	373,711.5	112,136,123	552.6	744.12	15.2
455	0450:55.710	5	3084	63.9	564,872	113,341,617	553.2	833.78	15.2
456	0451:01.710	3.35	3082	63.1	383,761.5	114,779,013	553.0	748.83	15.2
457	0451:07.710	5	3080	62.2	588,749	117,826,298	553.3	844.97	15.2
458	0451:13.710	3.35	3079	61.4	404,079	120,620,597	552.8	758.36	15.2
459	0451:19.710	5	3079	60.6	613,734	122,746,800	553.5	856.69	15.2
460	0451:25.710	3.35	3079	59.8	422,546	126,133,134	552.5	767.02	15.2
461	0451:31.710	5	3079	59.0	630,206.5	126,041,300	553.2	864.42	15.2
462	0451:37.710	3.35	3080	58.2	444,042.5	132,636,113	552.7	777.11	15.2
463	0451:43.710	5	3082	57.4	657,672.5	131,790,944	553.1	877.30	15.2
464	0451:49.710	3.35	3085	56.6	459,237	137,620,466	552.35	784.23	15.2
465	0451:55.710	5	3088	55.8	675,280.5	135,846,799	553.3	885.56	15.3
466	0452:01.714	3.35	3092	55.0	467,202	140,643,440	552.2	787.97	15.3
467	0452:07.714	5	3096	54.2	700,335.5	141,618,067	552.8	897.31	15.3
468	0452:13.714	3.35	3101	53.4	476,538.5	144,290,368	552.3	792.35	15.4
469	0452:19.718	5	3107	52.6	720,794	146,792,642	553.3	906.90	15.4
470	0452:25.714	3.35	3113	51.8	485,005	147,992,693	552.7	796.32	15.5
471	0452:31.714	5	3120	51.0	739,201	151,803,698	553.1	915.54	15.6
472	0452:37.714	3.35	3127	50.1	500,375.5	154,059,192	552.5	803.53	15.6
473	0452:43.718	5	3135	49.5	757,481	157,057,056	552.8	924.11	15.7
474	0452:49.718	3.35	3143	48.7	512,494.5	159,409,348	552.1	809.21	15.8
475	0452:55.714	5	3151	48.1	771,795.5	161,662,640	552.6	930.82	15.9
476	0453:01.714	3.35	3162	47.2	527,699.5	166,129,298	551.6	816.34	16.0

[a]4 hrs + m&s.

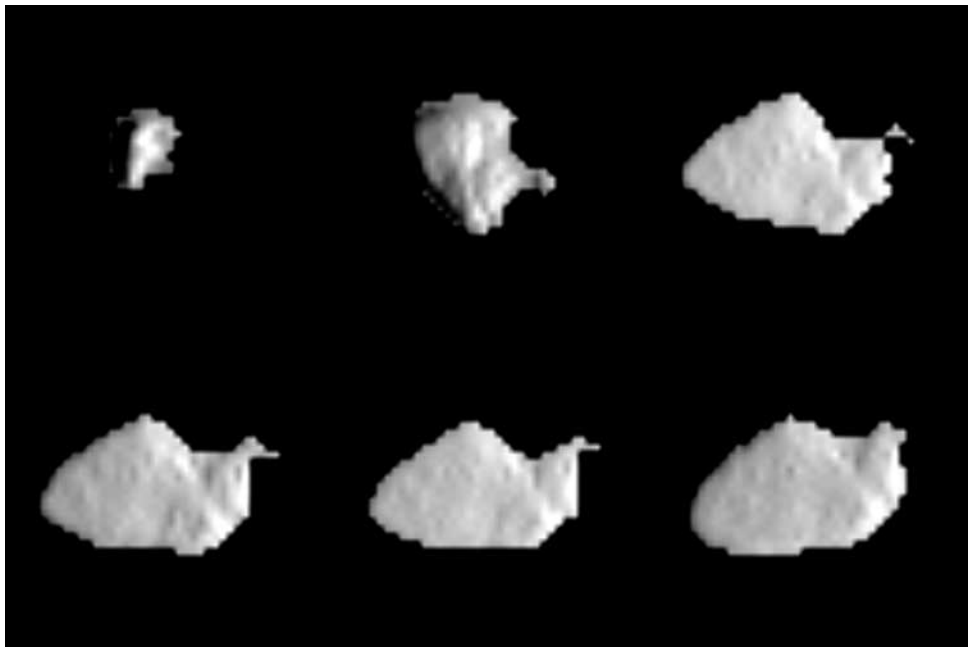

Figure 1. Six Annefrank images. From the upper left the images are numbers 401, 420, 454, 459, 464, and 474.

ground, hence the "missing" image numbers in Table 1, which lists every image actually transmitted to the ground. Memory capacity was not adequate to retain more than 72 images. Four images, taken before the software "locked" the spacecraft onto Annefrank and moved the asteroid to the center of the frame, were too near the edge of the field for good photometry. One image was lost, as expected, while the software was filtering the early data to provide proper locking coordinates. Four images were smeared due to inadequate settling time before long exposures. These can still be used for a measure of total image brightness. The flyby was totally successful in its major goal of uncovering potential problems before encountering P/Wild 2. Six of the images, in a processed form, are shown in Figure 1. The individual pixels become obvious near the edges where low-light-level pixels have been discarded to remove the scattered light halo. This process, when coupled with the low contrast caused by compression, also introduces some linear artifacts.

4. Image Processing

[5] A subimage pixel map, 100 × 100 pixels, was extracted from each image. The compressed data, which are nonlinear, were converted to the midpoint of their uncompressed equivalents, using a lookup function. A background was determined for each image from 1000 pixels well clear of the image. (This individual treatment was necessary, because the bias, which constitutes most of the background, decreases with camera use as the temperature of the electronics increases.) The background was subtracted from all 10,000 pixels in each subimage and these were then summed to give a measure of the total light from the asteroid, needed to determine the phase curve.

[6] Profiles were also run on each image in perpendicular directions in order to separate the true edge from the scattered light halo. It was assumed that extrapolation of the slope of the profiles above the halo to the background level gave a suitable measure of the edge location. A vertical profile across the middle of image 459 is shown in Figure 2.

[7] As might be expected, the brighter the asteroid image, the larger and brighter the scattered light halo. The slopes in Figure 2, for example, suggest the true limbs of the asteroid lie near pixels 41 and 59 and have a brightness of 900 dn. A least squares fit was made to the digital numbers (dn) at three or more apparent limb locations of each image, determined from two or more profiles, to the previously measured total brightness of those images. (The terminators were not used.) Since determinations from individual profiles tended to be somewhat subjective, the limb dn level for each image was therefore taken to correspond to the measured total image brightness in the least squares fit. An Excel countif function then was used to count the number of pixels brighter than that limb dn level to give a measure of the actual illuminated area for each image. This worked well for the brighter and larger images, but the earlier images contain so few pixels that their illuminated area is poorly determined.

[8] The final factor to be considered in attempting quantitative photometry is the absolute sensitivity of the camera. This was carefully measured for each pixel in the laboratory before launch, but the contamination that has plagued the camera from time to time has made these calibrations of limited value. A heating of the CCD to just above 0°C was carried out shortly before the Annefrank encounter. A few images of four stars taken shortly after the heating suggest that the Annefrank sensitivity is about 75% of that in the laboratory. This is based upon the dn level the stars should have had, given their spectral type, spectral class, parallax,

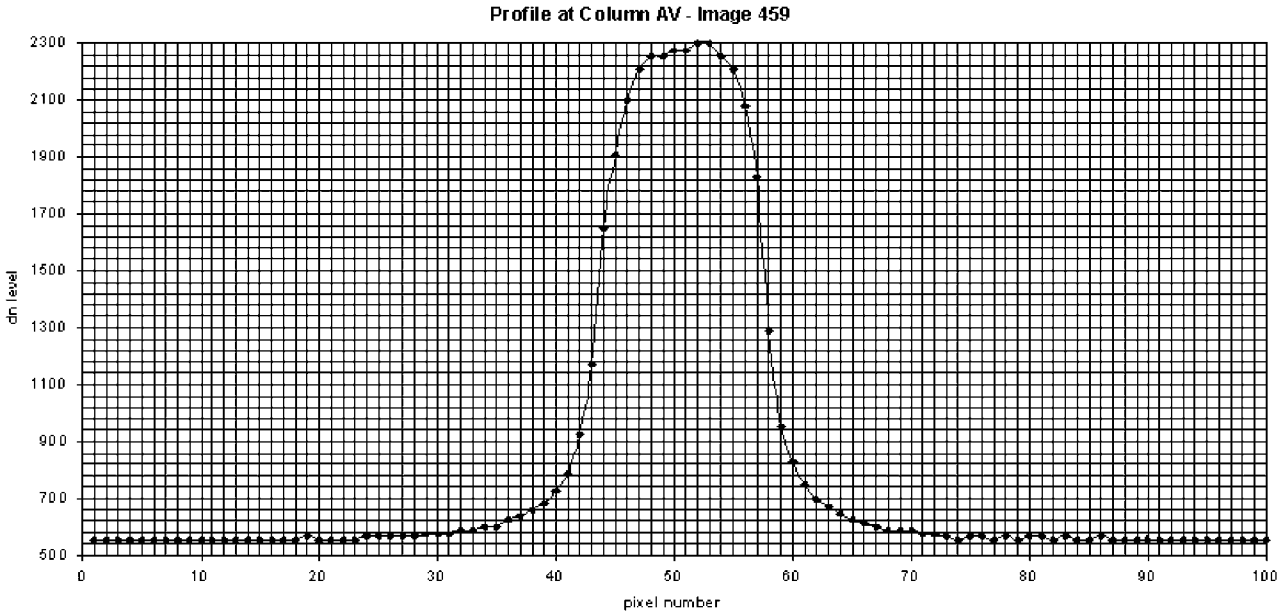

Figure 2. Profile of image 459 at column AV.

and V magnitude as given in the SIMBAD database. Additional images to improve this number are not yet available. The compressed background of the small subimages near the center of the field is quite constant, so the relative photometry of the camera is good, but the absolute calibration is quite suspect at this time.

5. Phase Curve

[9] The uncompressed and bias subtracted pixel brightness numbers can simply be summed to get a measure of the total flux in relative (dn) units. The total flux was then normalized to the distance of closest approach. Plotted against the phase angle, these give us a relative phase curve for Annefrank from 47° to 134°. Only one other asteroid, 253 Mathilde, a C-class, has ever been observed at phase angles larger than about 100°. Virtually all asteroid phase curves are nearly linear at small phase angles when plotted in semilog (magnitude versus angle) space, except for an opposition brightening [*Bowell et al.*, 1989]. Our Annefrank data were therefore extrapolated to zero phase with a 0.023 magnitudes per degree phase coefficient, the slope of our own data near 50°, and an 0.35 magnitude opposition effect. A point was arbitrarily interpolated at 90°. The resulting curve, produced by an ''Excel'' graphing program is shown as Figure 3. Observations by P. Weissman et al. (personal communication, 1999) and by R. Binzel (personal communication, 2000) suggest that Annefrank is an S-class asteroid and a slow rotator. All Stardust observations were taken in a 27 minute period, so clearly this curve is simply a curve at a particular rotational phase. (e.g., Annefrank's orientation was essentially fixed relative to the Sun.) The changing aspect of the asteroid in the images is due solely to the motion of the spacecraft past it. Whole disk photometry of the S-class asteroid 951 Gaspra acquired by the Galileo spacecraft showed a slightly larger phase coefficient (0.027) [*Helfenstein et al.*, 1994], while photometry of 433 Eros by NEAR showed a smaller value of 0.018 [*Domingue et al.*, 2002], but the latter required use of ground-based data for the smaller angles. Data have been reported only to 60° for Gaspra [*Helfenstein et al.*, 1994], 30° for Ida [*Helfenstein et al.*, 1996], and 90° for Eros [*Domingue et al.*, 2002]. NEAR did acquire a data point at 136° for the C-class asteroid 253 Mathilde [*Clark et al.*, 1999]. Mathilde had a geometric albedo of only 0.047 (at 700 nm) but showed a steep drop in its phase curve similar to Annefrank [*Clark et al.*, 1999].

[10] The change in illuminated area alone, assuming a circular profile [phase = $0.5(1 + \cos\alpha)$, where α is the phase angle], would have reduced the flux by only 1.87 magnitudes at 130° and 2.935 magnitudes at 150° relative to zero phase. The accompanying study (T. C. Duxbury et al., Size, shape, and spin state of mainbelt asteroid Annefrank, submitted to *Journal of Geophysical Research*, 2003) shows that the shape of Annefrank is certainly irregular and elongated, but the fractional change in illuminated area is not grossly different from that expected for a sphere. Clearly Annefrank is NOT a Lambert surface. It shows a drop of 5.7 magnitudes at 130°. This sharp drop in magnitude with increasing phase must be caused by some combination of changing cross section, shadowing, and a steep scattering law.

6. Albedo

[11] The Sun at 1 AU would present a value of 2.8808×10^{16} dn/s on the Stardust camera as it stood in the laboratory before launch. The measured illuminated area of the best images taken near closest approach to Annefrank is given in Table 1. There is a general trend showing increasing illuminated area as the phase decreases, but there are random fluctuations due largely to the poor photometric resolution of the compressed data. A compressed dn level might actually lie anywhere in a range of 14 uncompressed dn at the dn levels near image edges. Assuming the camera to be working at 75% of its laboratory level, as suggested by the few data taken immediately before the Annefrank

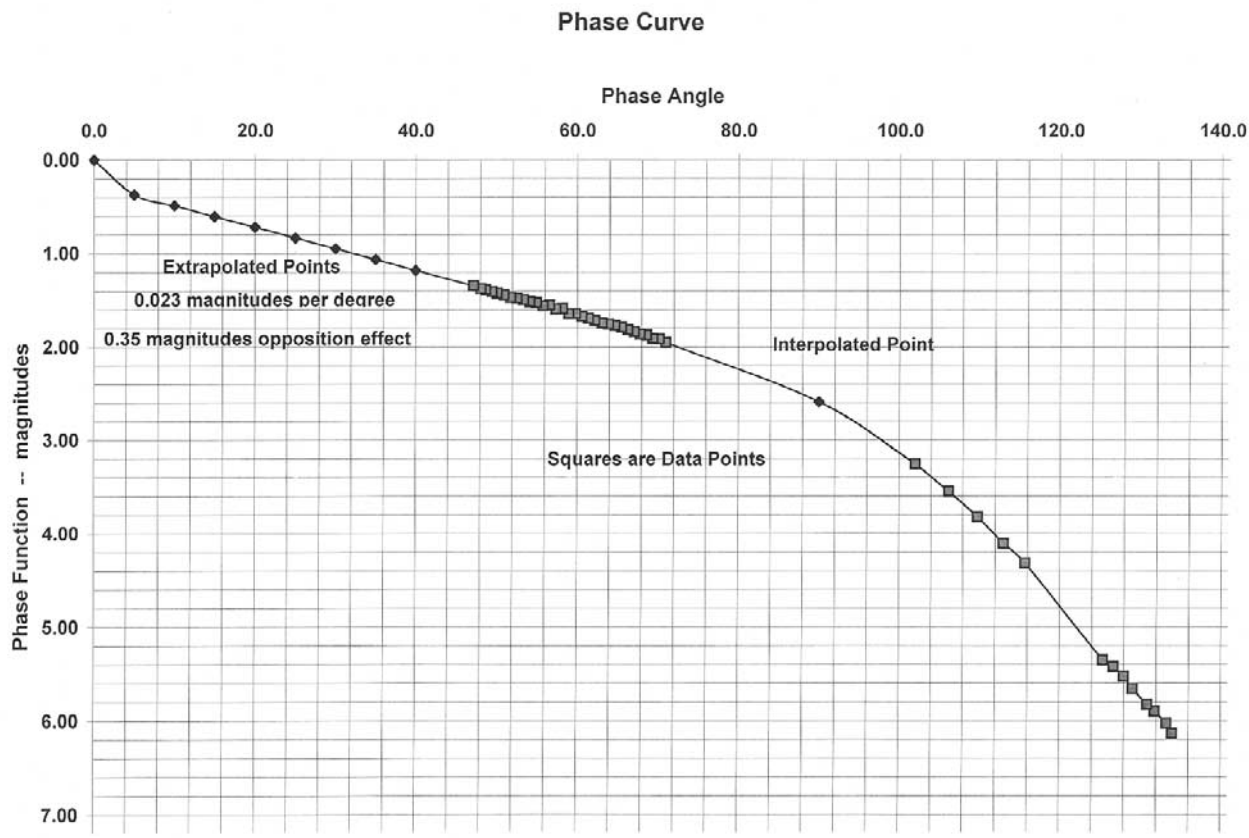

Figure 3. The Annefrank phase curve, normalized to closest approach.

encounter, the mean geometric albedo calculated for the measured data is 0.24. This was the mean value determined for all of the cross sections from 71° to 47° phase angle. If the camera were working at the laboratory level, these data would give an albedo value of 0.18. For comparison, the clear filter used by Galileo gave a result for the geometric albedo of Gaspra of 0.24 [*Helfenstein et al.*, 1994]. Integrated disk photometry of Eros by NEAR at 550 nm gave an albedo of 0.29 [*Domingue et al.*, 2002], while that for 243 Ida determined by Galileo was 0.206 [*Helfenstein et al.*, 1996]. Further checks of camera sensitivity, if made not too far in time from the Annefrank encounter, should improve our albedo value.

[12] The illuminated surface area determinations are independent of the camera sensitivity, however, and these will not change. A 16 km^2 illuminated ellipse seen broadside with two to one axial ratio would have radii of 1.6 and 3.2 km. Data from Hicks and Weissman [*Bowell et al.*, 1989] at a phase angle of 9.5° show a smaller illuminated cross section of 11.7 km^2, assuming 0.24 albedo, suggesting that the largest cross section of Annefrank was included in our best data. The data at the largest phase angles are difficult to interpret with any accuracy. The images consist of only a few pixels, so the areas are poorly determined and so are the total light levels, simply because of the large quantized steps in the data.

7. The Future

[13] These data will soon be available from the Planetary Data System. All images listed in the table will be included. Even images with some saturation can be useful for purposes such as study of areas near the limb where light levels are intrinsically low. Any further calibrations will also appear there. Anyone wishing to use the data should be very conscious of the presence of substantial scattered light and of the nonlinear nature of the dn values presented by the square root data compressor.

[14] **Acknowledgments.** We thank Mike Hicks, Paul Weissman, and Rick Binzel for their support of Stardust and for supplying observations to the Stardust project before their publication. All of the data used in this study are the result of dedicated efforts by the Stardust flight team at Lockheed Martin Astronautics and at the Jet Propulsion Laboratory of the California Institute of Technology. The Annefrank flyby was not a part of the nominal mission and was authorized very shortly before the event. We also wish to thank Mike A'Hearn and an anonymous reviewer for suggestions improving the clarity and accuracy of the paper. The analyses presented here were produced at the Jet Propulsion Laboratory, California Institute of Technology under contract to the National Aeronautics and Space Administration and sponsored by the Discovery Program.

References

Bowell, E., B. Hapke, D. Domingue, K. Lumme, J. Peltoniemi, and A. W. Harris, Application of photometric models to asteroids, in *Asteroids II*, pp. 524–556, Univ. of Arizona Press, Tucson, 1989.

Clark, B. E., et al., NEAR photometry of asteroid 253 Mathilde, *Icarus*, *140*, 53–65, 1999.

Domingue, D. L., et al., Disk-integrated photometry of 433 Eros, *Icarus*, *155*, 205–219, 2002.

Helfenstein, P., et al., Galileo photometry of asteroid 951 Gaspra, *Icarus*, *107*, 37–60, 1994.

Helfenstein, P., et al., Galileo photometry of asteroid 243 Ida, *Icarus*, *120*, 48–65, 1996.

Newburn, R. L., Jr., S. Bhaskaran, T. C. Duxbury, G. Fraschetti, T. Radey, and M. Schwochert, Stardust Imaging Camera, *J. Geo-*

phys. Res., *108*(E12), 8116, doi:10.1029/2003JE002081, in press, 2003.

S. Bhaskaran, R. S. Bhat, T. C. Duxbury, M. Hanner, E. E. Hirst, R. L. Newburn Jr., B. V. Semenov, P. Tsou, and T.-C. M. Wang, Jet Propulsion Laboratory, California Institute of Technology, 4800 Oak Grove Drive, Pasadena, CA 91109, USA. (shyam.bhaskaran@jpl.nasa.gov; ramachand.s.bhat@jpl.nasa.gov; tduxbury@jpl.nasa.gov; msh@mhanner.jpl.nasa.gov; edward.e.hirst@jpl.nasa.gov; ray.l.newburn@jpl.nasa.gov; boris.v.semenov@jpl.nasa.gov; peter.tsou@jpl.nasa.gov; tseng-chan.m.wang@jpl.nasa.gov)

G. R. Bollendonk, A. R. Cheuvront, D. E. Gingerich, S. J. Mumaw, K. A. Parham, and J. M. Vellinga, Lockheed Martin Astronautics, P.O. Box 179, Denver, CO 80201, USA. (gregory.r.bollendonk@lmco.com; allan.r.cheuvront@lmco.com; david.e.gingerich@lmco.com; susan.j.mumaw@lmco.com; kelly.a.parham@lmco.com; joseph.m.vellinga@lmco.com)

D. E. Brownlee, Department of Astronomy, University of Washington, Box 351580, Seattle, WA 98195, USA. (brownlee@astro.washington.edu)